21.1 A 65nm CMOS Living-Cell Dynamic Fluorescence Sensor with 1.05fA Sensitivity at 600/700nm Wavelengths

Fatemeh Aghlmand[1], Chelsea Hu[1,2], Saransh Sharma[1], Krishna K. Pochana[1], Richard M. Murray[1], Azita Emami[1]

[1]California Institute of Technology, Pasadena, CA
[2]Texas A&M University, College Station, TX

Integrated, low-cost and miniaturized devices that can detect clinically relevant biomarkers are crucial for the growing field of precision medicine as they can enable point-of-care diagnosis, continuous health monitoring and closed-loop drug delivery. Fluorescence (FL) sensing is known to be one of the most reliable, sensitive, and widely adopted sensing modality for many biomarkers [1,3]. However, detecting the weak FL signal requires complex optical setups, especially narrowband optical filters to block the strong excitation (EX) light. Prior efforts [1] to miniaturize and implement FL sensing in CMOS technologies have been limited to on-chip high-pass filters using dense vertical waveguide arrays. More importantly, the reported wavelength range of 800nm in [1] is not compatible with most of the commonly used fluorescent proteins that work with living cells [4]. Luminescence is another mechanism for detecting biomarkers that does not require an EX source and optical filtering [2]. However, there are limited number of luminescence proteins, and it is not feasible to use them in a closed-loop system since they can interfere with optogenetic control integration [5].

This work presents a fully integrated CMOS FL sensor to enable two-way communication between living cells and a CMOS chip using fluorescent proteins and optogenetic control. The sensor is not only capable of detecting static response of proteins but also can record the dynamic behavior of the cells, which is essential for implementing a closed loop system. This is achieved by continuously measuring the optical density (OD) and FL response of *E. coli* bacteria cells over the course of their growth. By providing appropriate optogenetic promoters, the sensor can modify the protein synthesis rate to approach the desired value. The proposed sensor can enable applications in smart medicine by detecting biomarkers for patients suffering from gut inflammatory diseases and aid in targeted drug delivery. Agricultural fields can also benefit from compact FL sensors when buried under the soil. A network of such low-power and wireless sensors connected to a central hub can locate areas with essential mineral deficiency for localized fertilization. The sensor (Fig. 21.1.1) includes optical filters, photodiodes (PD) and the processing circuitry on a single chip. A matched triple-well microfluidic (MF) chamber is designed to be closely assembled with the CMOS chip for differential measurement of the cultures in reference to each other, and with high sensitivity.

The most challenging task in integrating the FL sensor is to implement optical filters in standard CMOS process and in the wavelength range suitable for fluorescent proteins (<720nm). The filters need to be low-loss and robust against variation of light's polarization and angle of arrival (AoA). In recent years, periodic grating arrays based on surface plasmon polaritons (SPP) [6] have been used extensively to achieve narrowband optical filters. However, these filters are highly sensitive to the AoA while the cells in the MF chamber behave as unpolarized optical dipoles emitting in arbitrary directions. In this work, to enable passband filtering at shorter wavelengths, the high loss of Cu-SiO_2 interface is avoided by exploiting cavity modes [6]. Extensive FDTD simulations considering all 41 dielectric layers in the PDK, were performed to design and optimize the cavity arrays (Fig. 21.1.2). Such arrays show low dependency on AoA when sparse enough to avoid formation of strong propagating waves between the neighboring cavities. On the other hand, denser arrays are needed to achieve stronger signal. Optimization of these trade-offs resulted in 1D and 2D structures implemented using different metal layers (M7-M3, M7-M2) and dense via arrays (as vertical walls). The inner metal of the 2D coaxial cavity is only present in the last layer (instead of all layers) to make the filter both narrowband and low loss. The electric filed simulations in Fig. 21.1.2 verify that the field confinement in the narrow coaxial exit gap causes resonance (cavity modes).

Although 2D symmetric structures are more favorable for polarization-insensitive filters, the stringent DRC rules in CMOS do not allow for such 2D cavities in the 600nm range. Instead, 1D cavities are designed to transmit one of the polarizations (TE) and push the other one (TM) to the higher out-of-band range. As a result, the filter's collective in-band response is not affected by random light polarization. The cavity's minimum dimension, specifically the input/output gap size, is dictated by the DRC. Figure 21.1.2 shows that the field is confined inside the cavity which is filled with dielectric layers as opposed to the lossy Cu, producing a response at 600nm. A Psub/NW PD is designed as it has high responsivity in CMOS (Fig. 21.1.2). Taking advantage of silicon's wavelength dependent absorption coefficient, an N+/PW/DNW PD is also designed and optimized (using TCAD Synopsis tool). It provides additional filtering at 400nm while trading off responsivity. The optical measurements of selected filters and PDs using a 6nm BW unpolarized tunable light source are shown in Fig. 21.1.3.

In order to relax the stringent extinction-ratio requirement for the filter, another level of common mode filtering is implemented via a differential measurement scheme, as explained next (Fig. 21.1.4). The front-end features a C-TIA with variable switched capacitor gain, a voltage-controlled current source (VCCS), and feedback-controlled low-leakage switches to select between multiple inputs to the TIA. The FL signal is defined as EM_A/OD_A - EM_Φ/OD_Φ, where EM_A and EM_Φ are the emission (EM) responses of the cells with the fluorescent protein (A) and blank bacteria cells (Φ) respectively. The signal is measured differentially between the two cultures, and the cell measurement sensitivity is enhanced by subtracting a large part of the remaining background common-mode light. Finally, correlated double sampling (CDS) is applied to reduce the offset and low-frequency noise, and a resistive adder circuit is designed for collecting multiple PD/filter responses if necessary.

The measured output waveforms of the differential CDS and the responsivities of PD1 (Psub/NW) and the sensor at λ=700nm are shown in Fig. 21.1.4. The incident power is supplied by a tunable light source swept by a neutral density (ND) optical filter. The measured PD's responsivity is 0.024A/W and the sensor's responsivity (including 700nm filter and PD1) is 1.2mA/W. With integration time T_{int}=1s and using C_{TIA}=30fF, the sensor can detect 1.05fA of current with SNR >18dB. The most dominant noise source is the shot noise of the PD. The SNR can be improved by increasing T_{int}, which is limited by photobleaching of fluorescent proteins and the saturation of the front-end (Fig. 21.1.4). The latter is mitigated by using the variable C_{TIA} and the VCCS. The total output noise of the sensor is 3.846mV_{rms} under the dark condition, translating to an input-referred noise of 0.1154 fA_{rms}.

The biological measurement setup (Fig. 21.1.6) includes an MF well-holder, the EX LEDs (for FL), and the 600nm LED (for OD). Static and dynamic measurement results of the fluorescent proteins are shown in Fig. 21.1.5. miRFP protein, along with the equal OD blank cells, are loaded into a 5µL MF device and excited by a UV LED from the side. The FL EM is measured between the center (miRFP) and the right (blank) wells. To remove mismatches between the optical properties of the adjacent wells, a one-time calibration is done by recording the baseline when two wells are loaded with the same culture. Photobleaching is avoided by T_{int}=1s and using the maximum gain of the C-TIA (C_{TIA} =8fF). Detecting the presence of one fluorescent protein in a mixture of two is an important step in implementing a closed loop system, which needs at least one reporter and one reference biomarker. Two plasmids were co-transformed into *E. coli* cells to encode the expression of the mCherry and LSSmOrange proteins. Using appropriate chemical inducers in the growth media, either one or both of the proteins were expressed. The EM bands of these proteins lie in close proximity, while their EX wavelengths are distinct. Using two narrowband (FWHM=20nm) SMD LEDs, measurements are done to show that the sensor can distinguish two FL signals from a single bacterial strain that detects two different chemical signals (quorum sensing molecules) (Fig. 21.1.5).

Monitoring the dynamic growth and FL folding curve of the bacteria cells is another crucial step in implementing a two-way communication system. Super folder YFP (sfYFP) is selected due to its fast-folding response and widespread application. However, the optimum emission band of sfYFP is in lower 500nm range. Thanks to the high sensitivity of the integrated sensor, sfYFP is still measured at its non-optimum range of λ≥580nm using the combined response from the three PDs and the 600nm filters. sfYFP and blank cultures with initial OD=0.1 are loaded into a 10µL MF device and grown inside an incubator. The sensor measures the OD of each culture by emitting 600nm light once every 20 minutes. Based on the Beer-Lambert's law, the cells absorb and scatter more light as they grow, resulting in less light reaching the PD. Over the growth time, fresh media is pumped very slowly (0.5µL/hr) into the wells to provide the cells with the required nutrition and oxygen.

The die micrograph of the chip implemented in 65nm CMOS is shown in Fig. 21.1.7. The comparison table shows that to the best of our knowledge, this work is the first integrated FL sensor capable of measuring static and dynamic cell responses and can enable the control of the dynamic behavior of living bacteria cells with fluorescent proteins.

Acknowledgement:
This work was supported by the Institute for Collaborative Biotechnologies through contract W911NF-19-D-0001 from the U.S. Army Research Office, and by the Center for Sensing to Intelligence (S2I) at Caltech.

References:
[1] L. Hong et al., "Fully Integrated Fluorescence Biosensors On-Chip Employing Multi-Functional Nanoplasmonic Optical Structures in CMOS," *IEEE JSSC,* vol. 52, no. 9, pp. 2388–2406, Sep. 2017.
[2] Q. Liu et al., "A Threshold-Based Bioluminescence Detector With a CMOS-Integrated Photodiode Array in 65 nm for a Multi-Diagnostic Ingestible Capsule," *IEEE JSSC,* 2022, doi: 10.1109/JSSC.2022.3197465.
[3] E. P. Papageorgiou et al., "Chip-Scale Angle-Selective Imager for In Vivo Microscopic Cancer Detection," *IEEE TBioCAS,* vol. 14, no. 1, pp. 91-103, Feb. 2020.

 978-1-6654-9016-0/23/$31.00

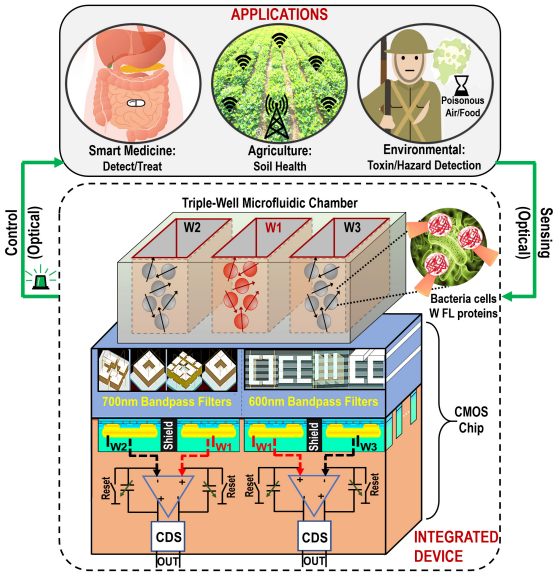

Figure 21.1.1: Block-level diagram of the integrated CMOS Fluorescence sensor and its applications.

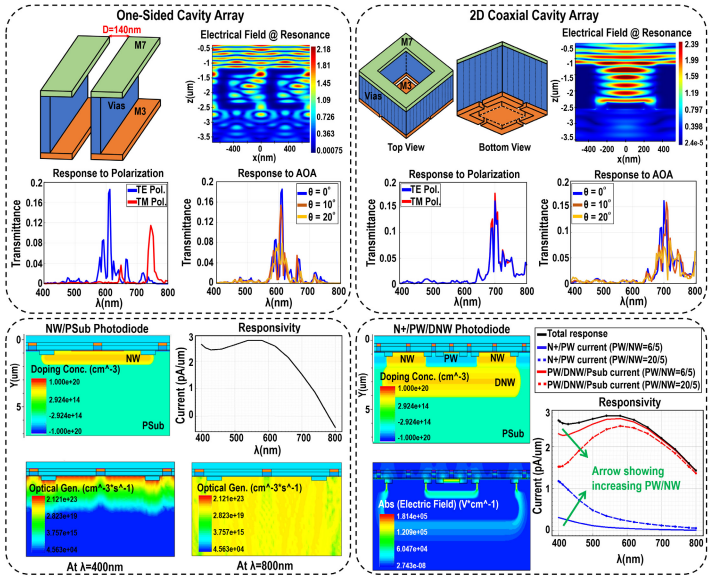

Figure 21.1.2: Design and simulation results of one-sided and 2D coaxial cavity arrays (top); NW-Psub (PD1) and N+/PW/DNW (PD2) (bottom).

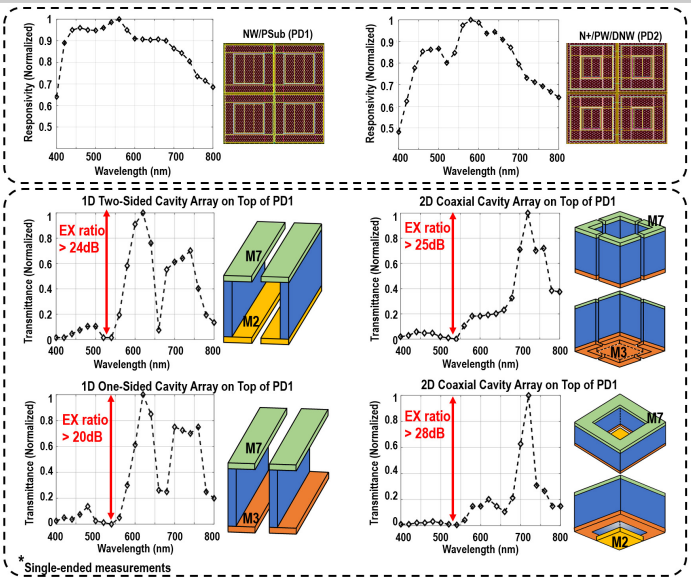

Figure 21.1.3: Measured response of bare PD1 and PD2 (top); measured response of the cavity array optical filters on top of PD1 (bottom).

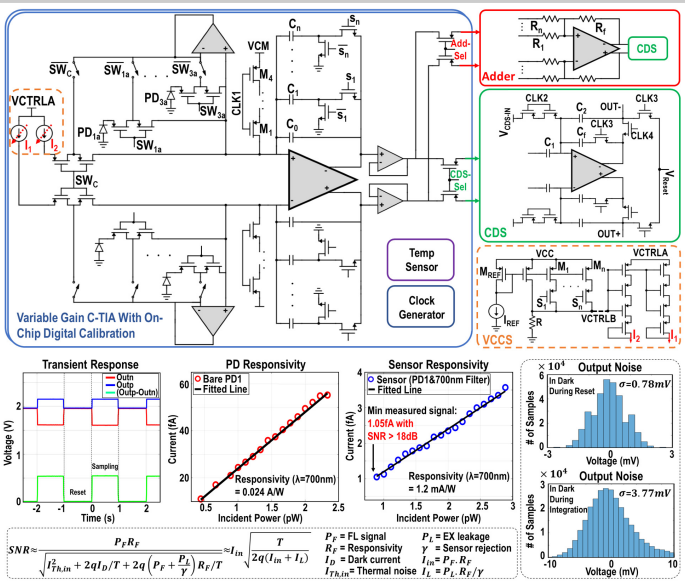

Figure 21.1.4: Circuit design of the FL sensor (top); measured results of the sensor and SNR definition (bottom).

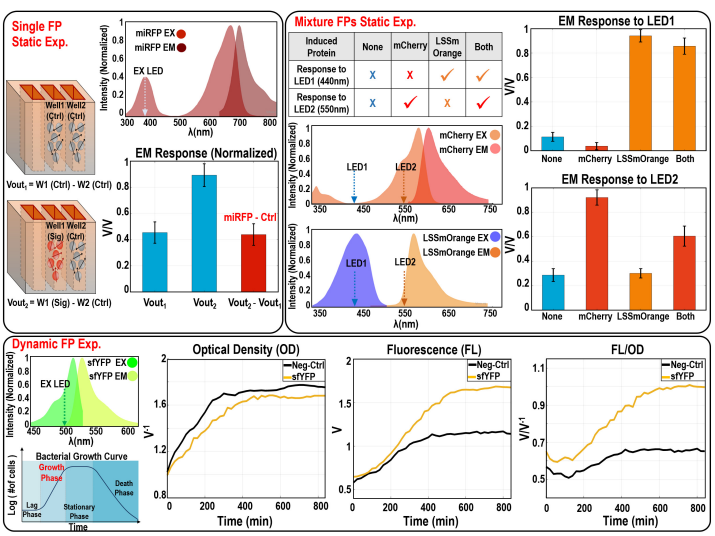

Figure 21.1.5: Measured static response of single and mixture FPs (top); dynamic measurement results of *E. coli* bacteria cells with sfYFP (bottom).

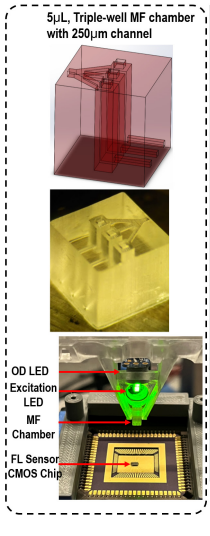

Metric	[1] JSSC '2017	[2] JSSC '2022	[3] TBioCAS'2020	This Work
Technology	65nm	65nm	180nm	**65nm**
Detector Type	Fluorescence	Bioluminescence	Fluorescence	**Fluorescence**
Optical Filter (CMOS)	Yes (High-pass)	No	No	**Yes (Band-pass)**
Reporter Type	Qdot800 tags	Luminescence protein in bacterial cells	Qdot705 tags	**miRFP, LSSmOrange, mCherry, sfYFP in bacterial cells**
Measurement Type	Static	Static/Dynamic	Static	**Static / Dynamic (OD and FL signals)**
Excitation Source	405nm laser	N.A.	Laser (Blue)	**SMD LED**
PD Active Area	91.4 x 123 μm²	1.24 x 1.24 mm²	55 x 55 μm²	**100 x 100 μm²**
PD/Pixel Responsivity	22 mA/W (PD at 780nm)	N.R.	90.2 mA/W # (Pixel)	**24 mA/W (PD at 700nm)**
Power	66mW *	16.3μW **	3.5mW ***	**Single Row:7.05mW $ Three Rows:19.1mW $$**
Output Noise ##	1.31mV_{rms}	N.R.	4.5mV_{rms}	**3.846mV_{rms}**
Sensor Sensitivity	0.33fA	59fA	N.R.	**1.05fA**
Integration time	1-10s	25.8s	10-50ms	**1s**
SNR	>20dB	N.R.	15.5dB	**18.3dB**

* Converted from reported pixel responsivity of 8.2V/pW.s, using Cfb=11fF and Tin=50ms.
** Total capsule power for 2x2 array (Wireless)
*** Reported for 80 x 36 pixels array
\# Reported for dual sensors
Under dark condition
$ Includes 1x (C-TIA + 4 buffers + 1/3 of a shared CDS) for 4 pixels
$$ Includes 3x (C-TIA + 4 buffers) + 1x CDS for 12 pixels
N.A. – Not Applicable
N.R. – Not Reported

Figure 21.1.6: Bio-measurement setup (left); comparison of the integrated FL sensor with state-of-the-art sensors and systems (right).

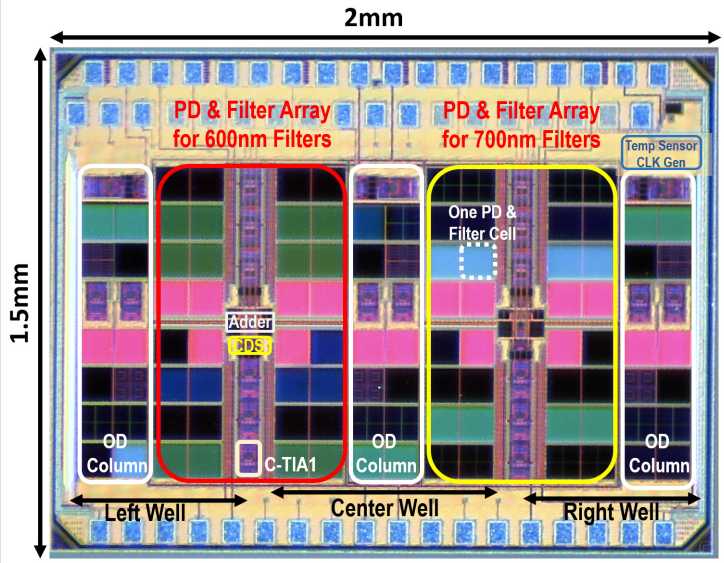

Figure 21.1.7: 65nm CMOS chip micrograph.

Additional References:

[4] E. A. Rodriguez et al., "The Growing and Glowing Toolbox of Fluorescent and Photoactive Proteins," *Trends in Biochemical Sciences,* vol. 42, no. 2, pp. 111-129, Feb. 2017.

[5] N. T. Ong and J. J. Tabor, "A Miniaturized Escherichia coli Green Light Sensor with High Dynamic Range," *European Journal of Chemical Biology,* vol. 19, no. 12, pp. 1255-1258, Jun. 2018.

[6] E. Popov et al., "Enhanced Transmission Due to Non-plasmon Resonances in One and Two-Dimensional Gratings," *Applied Optics,* vol. 43, no. 5, pp. 999-1008, 2004.

978-1-6654-9016-0/23/$31.00